JACS
JOURNAL OF THE AMERICAN CHEMICAL SOCIETY
Article
pubs.acs.org/JACS

Equatorenes: Synthesis and Properties of Chiral Naphthalene, Phenanthrene, Chrysene, and Pyrene Possessing Bis(1-adamantyl) Groups at the Peri-position

Koji Yamamoto, Naohiro Oyamada, Sheng Xia, Yuta Kobayashi, Masahiko Yamaguchi,* Hiroaki Maeda,[†] Hiroshi Nishihara,[†] Tadafumi Uchimaru,[‡] and Eunsang Kwon[§]

Department of Organic Chemistry, Graduate School of Pharmaceutical Sciences, Tohoku University, Aoba, Sendai, 980-8578, Japan
[†]Department of Chemistry, School of Science, The University of Tokyo, Hongo, Bunkyo, Tokyo, 113-0033, Japan
[‡]Nanosystem Research Institute, AIST, Tsukuba, Ibaraki, 305-8568, Japan
[§]Research and Analytical Center for Giant Molecules, Tohoku University, Japan

Supporting Information

ABSTRACT: Chiral polycyclic aromatic hydrocarbons containing bis(1-adamantyl) groups at the peri-positions, named equatorenes, were synthesized in optically pure form starting from optically pure 4,5-bis(1-adamantyl)-8-methoxy-1-naphthol. A sequential Diels–Alder reaction of furan and arynes generated from 1,2-bromotriflates provided tricyclic and tetracyclic epoxides, and acid-catalyzed aromatization gave phenanthrol and chrysenol. Deoxygenation reactions involving the hydrogenolysis of triflates gave 1,8-bis(1-adamantyl)-naphthalene, 1,10-bis(1-adamantyl)phenanthrene, and 1,12-bis(1-adamantyl)chrysene. 3,4-Bis(1-adamantyl)pyrene was synthesized from phenanthrol by Sonogashira coupling and Pt-catalyzed cyclization. Essentially no racemization occurred during the synthesis. X-ray analysis indicated the distorted naphthalene moiety possessing the peri-diadamantyl groups and the flat structure of the other benzene rings. UV–vis analysis of the equatorenes showed considerable redshifts compared with that of the corresponding achiral arenes. Electrochemical analysis of the naphthalene and pyrene indicated that the distortion decreased the highest occupied molecular orbital stability with no marked effect on the lowest unoccupied molecular orbital energy level, and the origin was discussed on the basis of calculation results.

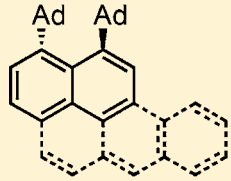

INTRODUCTION

Polycyclic aromatic hydrocarbons (PAH) are produced as raw or pure materials in large quantities, and exploring their properties is an important subject in organic chemistry as a basis for the development of functional materials and biologically active substances.[1] Many aromatic compounds have planar sp^2 carbon structures, often with some protons bound at the peri-positions, and π-electrons on both sides of their aromatic plane play critical roles in their reactivity and properties. It is thus interesting to obtain chiral polycyclic aromatic hydrocarbons by introducing distortions into the aromatic system, since distorted π-systems can exhibit properties not shown by achiral derivatives. Helicenes, which contain an *o*-condensed polycyclic arene skeleton for inducing helical chirality, have been examined for chiral aromatic hydrocarbons.[2] Their structure diversity, however, is limited because of the intrinsic *o*-condensed rings, but a fusion with other structures or rings partly alleviate this drawback.[3] In this regard, several distorted non-*o*-condensed chiral polycyclic arenes, particularly 1,8-disubstituted naphthalenes,[4−6] and related compounds,[7,8] have been examined. Although these compounds had chiral structures, they could not be resolved because of their low activation barrier of racemization. Thus, a general method of providing chiral arenes with sufficient thermal stability to racemization is desired, which, for example, will provide optically active naphthalenes and pyrenes.

We previously developed chiral naphthalene derivatives with 1,8-bis(1-adamantyl) groups, which do not racemize at ambient temperature.[9] In this study, several chiral polycyclic aromatic hydrocarbons were synthesized using the chirality exerted by the bis(1-adamantyl) group at the peri-position: 1,8-bis(1-adamantyl)naphthalene **1**, 1,10-bis(1-adamantyl)phenanthrene **2**, 1,12-bis(1-adamantyl)crysene **3**, and 3,4-bis(1-adamantyl)-pyrene **4** were synthesized in racemic and optically pure forms (Figure 1). Such compounds were named equatorenes, which have distorted structures at the equator plane of the molecules. Spectroscopic and electrochemical analyses along with DFT calculations were conducted to compare racemic, optically active, and achiral arenes, which revealed notable physical properties of equatorenes.

Received: July 29, 2013
Published: October 2, 2013

dx.doi.org/10.1021/ja407800e | J. Am. Chem. Soc. 2013, 135, 16526–16532

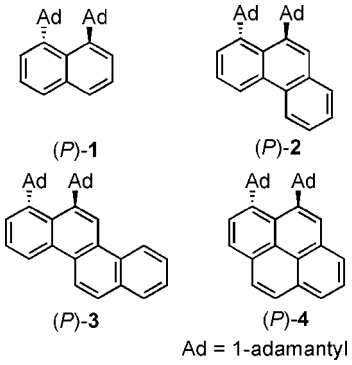

Figure 1. Structures of equatorenes.

SYNTHESIS

The synthesis of chiral polycyclic aromatic hydrocarbons started from known (*P*)-4,5-bis(1-adamantyl)-8-methoxy-1-naphthol (*P*)-**5**, which was synthesized from 6-(1-adamantyl)-3-(*t*-butyldimethylsilyloxy)-2-iodophenyl trifluoromethanesulfonate and 2-(1-adamantyl)furan in five steps in 19% overall yield containing an optical resolution in multigram quantities.[9] The aryne Diels–Alder reaction was employed to extend the π-system from bicyclic naphthalene to tricyclic phenanthrene and tetracyclic chrysene.

The bromination of (*P*)-**5** with benzyltrimethylammonium tribromide[10] gave the bromonaphthol (*P*)-**6**, which was converted to the triflate (*P*)-**7** (Scheme 1). Aryne generation

Scheme 1. Synthesis of Phenanthrol (*P*)-9 and Chrysenol (*P*)-13

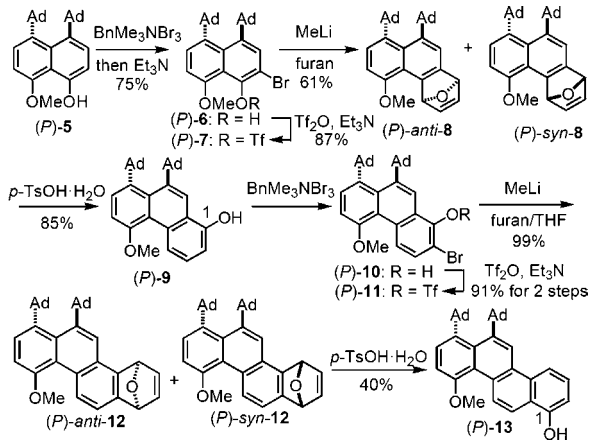

with methyllithium and the Diels–Alder reaction in furan solvent were conducted giving the tricyclic epoxide (*P*)-**8** as a separable mixture of two diastereomers in 1:1 ratio in the yield of 61%. The treatment of the isomeric mixture of (*P*)-**8** with *p*-toluenesulfonic acid provided the phenanthrol (*P*)-**9** in 85% yield. The presence of a hydroxy group at the 1-position was determined by nuclear Overhauser effect (NOE) studies. Then, another sequence of bromination, triflation, and aryne Diels–Alder reaction in furan-THF (1:1) gave the tetracyclic epoxide (*P*)-**12** as a 1:1 mixture of diastereomers. The acid treatment of (*P*)-**12** gave chrysenol (*P*)-**13** in 40% yield. The hydroxy group at the 1-position was determined by NOE experiments. Starting from racemic (±)-**5**, a racemic series of the tri- and tetracyclic compounds (±)-**9** and (±)-**13** were obtained. The regioselectivity in the acid-catalyzed ring-opening may be explained by the stability of the benzyl carbocation intermediates formed by the ring-opening.

Then, the above polycyclic compounds **5**, **9**, and **13** in racemic and (*P*)-forms were converted to the corresponding hydrocarbons by the hydrogenolysis of triflates. The naphthol (*P*)-**5** was demethylated with boron tribromide giving the ketol (*P*)-**14** in 50% yield (Scheme 2). Probably because of the steric

Scheme 2. Synthesis of Optically Active (*P*)-1

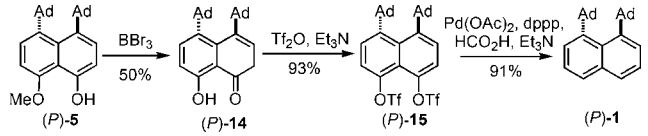

repulsions and aromatic ring tension exerted by the peri-bis(1-adamantyl) groups, (*P*)-**14** was obtained in keto form. Reaction of (*P*)-**14** with triflic anhydride gave the bistriflate (*P*)-**15** in 93% yield, which was subjected to hydrogenolysis using formic acid in the presence of palladium acetate, and optically active (*P*)-**1** was obtained in 91% yield. HPLC analysis indicated >95% ee (Supporting Information, Figure S2), and no racemization occurred during the keto–enol interconversion and hydrogenolysis. Racemic (±)-**1** was synthesized from (±)-**14**, which was obtained from 1,8-di(1-adamantyl)-5-(*tert*-butyldimethylsilyloxy)-1,4-dihydro-1,4-epoxynaphthalene[9] by the removal of the silyl protecting group and acid treatment.

The removal of the oxygen functional groups in the phenanthrol (*P*)-**9** was conducted by stepwise hydrogenolysis (Scheme 3). The hydroxy group in (*P*)-**9** was reduced via

Scheme 3. Synthesis of Optically Active (*P*)-2

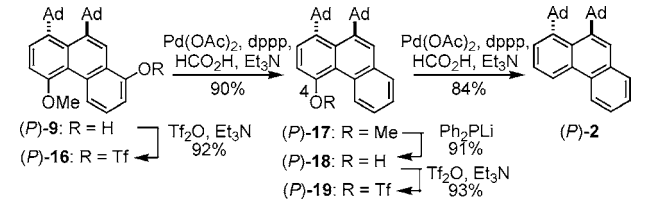

triflate giving the 4-methoxyphenanthrene (*P*)-**17**. Then, demethylation,[11] triflation, and hydrogenolysis provided (*P*)-**2**. Essentially no racemization was observed as indicated by 99% ee of (*P*)-**2** (Supporting Information, Figure S3). Racemic (±)-**2** was obtained by the same method starting from (±)-**9**. Using the same method, the chrysenols (*P*)-**13** and (±)-**13** were deoxygenated giving the chrysenes (*P*)-**3** and (±)-**3**, respectively (Scheme 4).

The chiral pyrenes (*P*)-**4** and (±)-**4** were synthesized from (*P*)-**19** and (±)-**19**, respectively (Scheme 5). The Sonogashira coupling with trimethylsilylacetylene, and deprotection gave the 4-ethynylphenanthrenes (*P*)-**25** and (±)-**25**. Then, platinum-

Scheme 4. Synthesis of Optically Active (*P*)-3

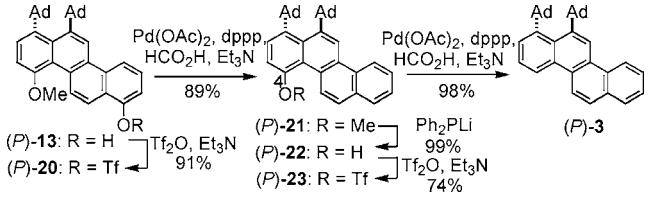

dx.doi.org/10.1021/ja407800e | J. Am. Chem. Soc. 2013, 135, 16526–16532

Scheme 5. Synthesis of Optically Active (*P*)-4

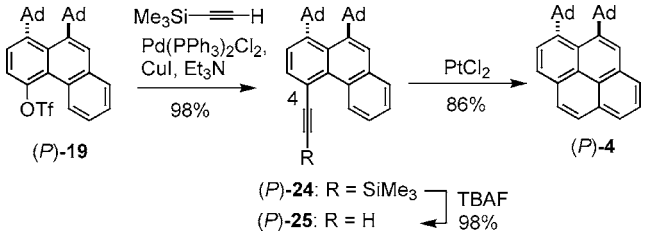

catalyzed cyclization[12] gave (*P*)-**4** and (±)-**4**. The optical purity >99% ee of (*P*)-**4** was determined by HPLC analysis (Supporting Information, Figure S5).

The sequential expansion of the aromatic ring system using the aryne Diels–Alder reaction converted the chiral naphthalene **5** to the phenanthrene **2**, the chrysene **3**, and the pyrene **4** without racemization. Four chiral polycyclic arenes, all equatorenes, in racemic and optically pure forms were obtained, and their properties were compared with the properties of naphthalene, phenanthrene, chrysene, and pyrene to determine the effect of the distorted aromatic π-systems. Note that the chiral version of all the polycyclic aromatic hydrocarbons can, in principle, be obtained by introducing the bis(1-adamantyl) group at the peri-position, and that chiral arenes do not racemize under ambient conditions.

With regard to the thermal stability of the equatorenes, kinetic studies on racemization in *o*-dichlorobenzene were conducted to obtain the rate constants (k) and half-lives ($T_{1/2}$) (Table 1). The $T_{1/2}$ for (*P*)-**2**, (*P*)-**3**, and (*P*)-**4** at 120 °C were

Table 1. Rate Constants (sec^{-1}) and Half-Lives (min) of (*P*)-1 (70 °C), (*P*)-2, (*P*)-3, and (*P*)-4 (120 °C) in *o*-Dichlorobenzene (0.02 mM)

compound	temp (C°)	$k/10^{-4}$ (sec^{-1})	$T_{1/2}$ (min)
(*P*)-**1**	70	2.0	58
(*P*)-**2**	120	2.5	46
(*P*)-**3**	120	2.6	44
(*P*)-**4**	120	0.85	140

longer than 40 min (Supporting Information, Figures S7, S8, and S9). The stability of (*P*)-**1** was lower, and $T_{1/2}$ 58 min was obtained at 70 °C (Supporting Information, Figure S6). The order of the configurational stability (*P*)-**1** < (*P*)-**2** ≈ (*P*)-**3** < (*P*)-**4** increased with the number of benzene rings attached to 1,8-bis(1-adamantyl)naphthalene core. The results showed that the compounds (*P*)-**1**, (*P*)-**2**, (*P*)-**3**, and (*P*)-**4** can be treated by usual manipulations at ambient temperature.

■ CRYSTAL STRUCTURES

X-ray analysis[13] of (±)-**1** exhibited a distorted naphthalene ring with two 1-adamantyl groups directed to both sides of the π-plane (Figure 2) with a dihedral angle, C19–C8–C1–C9, of 71.6°. C1 and C8 in the naphthalene ring at the peri-position were separated by 0.090 nm above and below the naphthalene mean plane, and the adamantyl carbons C9 and C19 were separated by 0.282 nm. The angles C7–C8–C8a and C8–C8a–C4a were 117° and 116°, respectively, with only a slight distortion from the achiral naphthalene with 120°, which indicated that the aromatic system was maintained. The packing structure in the crystal showed that the adamantyl groups are faced toward the aromatic rings of other molecules,

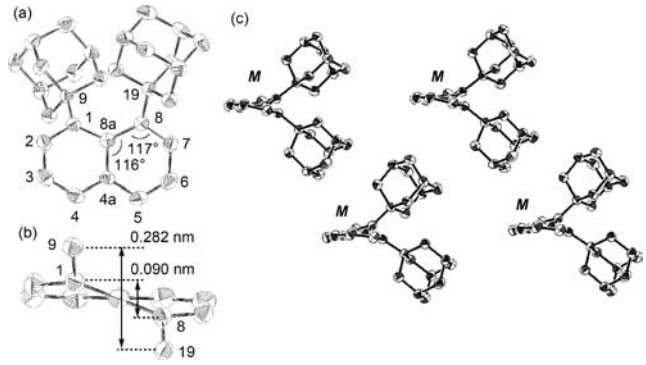

Figure 2. Thermal ellipsoid plot of (±)-**1** (a and b) at 50% probability. Hydrogen atoms are omitted for clarity. Two adamantyl groups are removed for clarity in panel b. The packing structure of (±)-**1** in the crystal is also shown (c).

which was generally observed in equatorenes, as will be shown in (±)-**2**, (±)-**3**, and (±)-**4**.

The A and B rings of the phenanthrene (±)-**2** obtained by X-ray analysis were similar to those of naphthalene (±)-**1** with a dihedral angle, C11–C1–C10–C21, of 76.0° (Figure 3). The

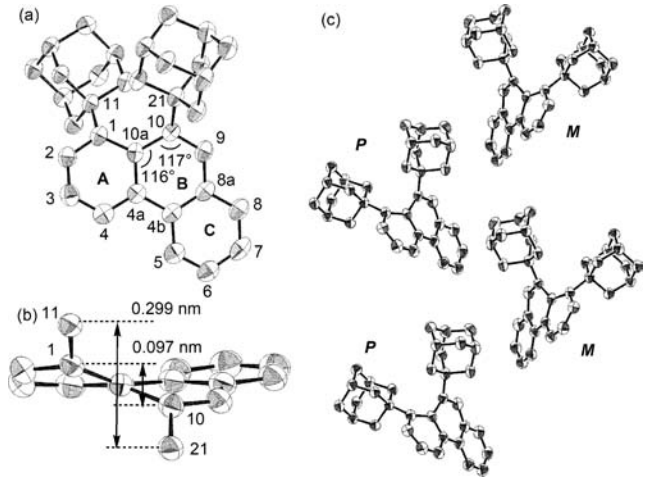

Figure 3. Thermal ellipsoid plot of (±)-**2** (a, b) at 50% probability. Hydrogen atoms are omitted for clarity. Two adamantyl groups are removed for clarity in panel b. The packing structure of (±)-**2** in the crystal is also shown (c).

C ring had a flat structure, which was confirmed from the sum of the internal angles of the C ring of 720°. C1 and C10 in A and B rings, and the adamantyl carbons C11 and C21 lay above and below the mean plane by 0.097 nm, and 0.299 nm, respectively, which were again similar to those of (±)-**1**.

The X-ray structure of the chrysene (±)-**3** in the naphthalene moiety showed a similar tendency to those of (±)-**1** and (±)-**2** with a dihedral angle, C13–C1–C12–C23, of 79.2° (Figure 4). The distances between C1 and C12, and between the adamantyl carbons C13 and C23 were 0.103 and 0.309 nm, respectively. The C and D rings had flat structures.

The X-ray structure of the pyrene (±)-**4** showed similar distortions at the A and B rings attached to the adamantyl group and flat structures at the C and D rings (Figure 5). A dihedral angle, C11–C3–C4–C21, of 77.8° was observed, which was similar to those of (±)-**1**, (±)-**2**, and (±)-**3**. The distances C3/C4 and C11/C21 were 0.097 and 0.300 nm, respectively.

dx.doi.org/10.1021/ja407800e | J. Am. Chem. Soc. 2013, 135, 16526–16532

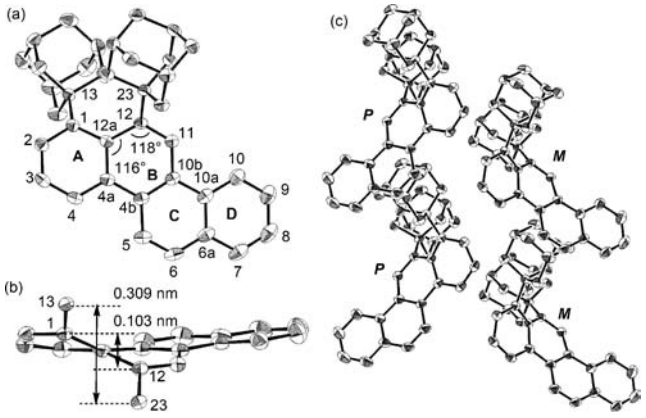

Figure 4. Thermal ellipsoid plot of (±)-**3** (a, b) at 50% probability. Solvent molecules (2,2,5,5-tetramethyltetrahydrofuran) and hydrogen atoms are omitted for clarity. Two adamantyl groups are removed for clarity in panel b. The packing structure of (±)-**3** in the crystal is also shown (c).

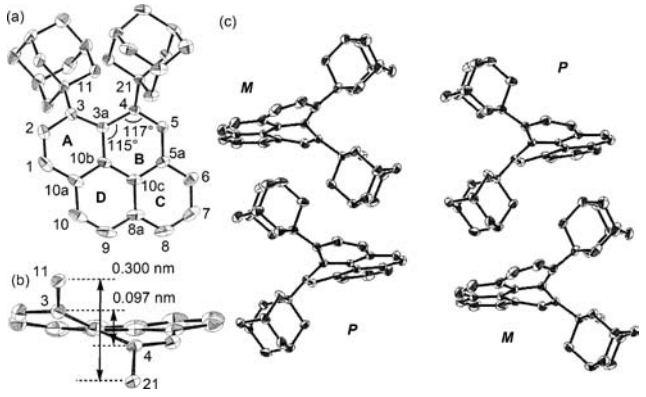

Figure 5. Thermal ellipsoid plot of (±)-**4** (a and b) at 50% probability. Hydrogen atoms are omitted for clarity. Two adamantyl groups are removed for clarity in panel b. The packing structure of (±)-**4** in the crystal is also shown (c).

Generally, equatorenes have a distorted naphthalene moiety attached to their bis(1-adamantyl) groups and a flat structure at other aromatic rings. This may be common in other equatorene families.

SPECTROSCOPIC PROPERTIES

UV−vis analyses exhibited a notable feature of equatorenes. Racemic and optically pure (*P*)-**1** and (±)-**1** in ethanol provided an absorption maximum at 323 nm (ε 5.7 × 10^3 $M^{-1}cm^{-1}$), which was in contrast to the considerably shorter wavelengths of the absorption maximum for naphthalene and 1,8-dimethylnaphthalene at 264 and 285 nm, respectively (Figure 6). Thus, the distortion of the aromatic system induced a 60 nm redshift in **1**. Related redshifts were observed for 1,8-di-(*t*-butyl)naphthalene[4a] and a cyclophane naphthalene,[8b] but **1** exhibited a considerably larger redshift.

The chiral phenanthrene **2**, the chrysene **3**, and the pyrene **4** also exhibited redshifts of 40 nm by UV−vis (Figure 7 and Supporting Information, Figures S10 and S12). The redshifts appear to be a common phenomenon in equatorenes.

CD spectra of (*P*)-**1**, (*P*)-**2**, (*P*)-**3**, and (*P*)-**4** showed negative Cotton effects between 300 and 350 nm (Figure 8). The fluorescence for the chiral equatorenes was very weak in solution and solid state compared with that for the achiral

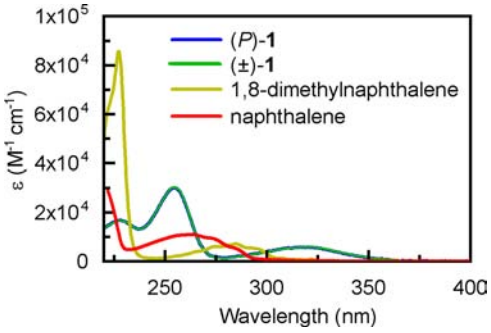

Figure 6. UV−vis spectra (0.1 mM, 25 °C, EtOH) of naphthalene derivatives. Blue and green lines are overlapped.

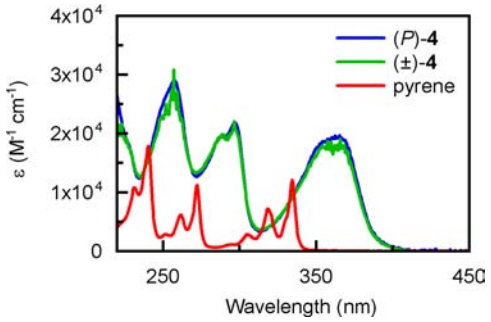

Figure 7. UV−vis spectra (0.1 mM, 25 °C, cyclohexane) of pyrene derivatives.

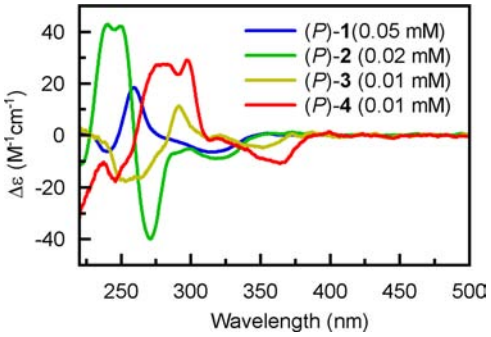

Figure 8. CD spectra (cyclohexane, 25 °C) of diadamantyl aromatic hydrocarbons.

arenes (Figure 9and Supporting Information, Figures S11, S13, and S14). Since 2-(1-adamantyl)naphthalene was reported to be highly fluorescent,[14] the observation may not be due to the presence of the adamantyl group but to the distorted π-system.

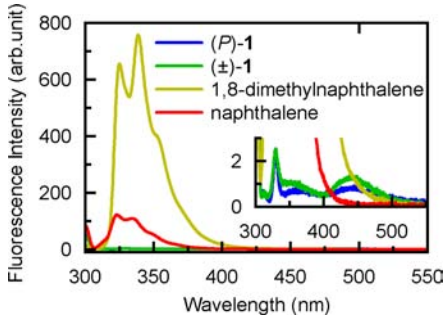

Figure 9. Emission spectra (0.1 mM, ethanol, 25 °C, λ_{ex} = 300 nm) of naphthalene derivatives. The inset shows enlarged spectra.

dx.doi.org/10.1021/ja407800e | *J. Am. Chem. Soc.* 2013, 135, 16526−16532

Table 2. Oxidation and Reduction Potentials of Naphthalene Derivatives in 0.1 M n-Bu_4NClO_4/Acetonitrile Solution

	E_1[a] (V vs Fc^+/Fc)	E_2[a] (V vs Fc^+/Fc)	$E_2 - E_1$ (V)	difference from naphthalene (V)
naphthalene	−2.99	1.23	4.21	0
1,8-dimethylnaphthalene	−3.09	1.05	4.14	−0.07
(±)-**1**	−2.94	0.81	3.75	−0.46
(*P*)-**1**	−2.94	0.82	3.76	−0.45

[a]Determined by DPV.

ELECTROCHEMICAL PROPERTIES

The oxidation and reduction potentials of the chiral naphthalenes (*P*)-**1** and (±)-**1** were compared with those of naphthalene using cyclic voltammetry (CV) and differential pulse voltammetry (DPV) in 0.1 M n-Bu_4NClO_4/acetonitrile solution (Table 2). It was observed that (*P*)-**1** and (±)-**1** gave the same oxidation and reduction waves of E_1 = −2.94 V for (*P*)-**1** and −2.94 V for (±)-**1**, and E_2 = 0.82 V for (*P*)-**1** and 0.81 V for (±)-**1**, respectively, referenced to the redox potential of ferrocenium/ferrocene (Fc^+/Fc). For comparison, naphthalene provided E_1 = −2.99 V and E_2 = 1.23 V. Note that **1** and naphthalene exhibited similar E_1 values but different E_2 values, and that distortion facilitated oxidation with reduction remaining relatively unchanged: The distortion destabilized the highest occupied molecular orbital (HOMO) energy level but hardly affected the lowest unoccupied molecular orbital (LUMO) energy level. The $E_2 - E_1$ values of 3.76 V for (*P*)-**1**, 3.75 V for (±)-**1**, and of 4.21 V for naphthalene indicated that the distortion decreased $E_2 - E_1$ by 0.45−0.46 V.

Electrochemical analysis was also conducted for pyrenes (Table 3). The compounds (*P*)-**4** and (±)-**4** gave the same oxidation and reduction waves of E_1 = −2.57 V and E_2 = 0.62 V, respectively. Compared with pyrene with E_1 = −2.53 V and E_2 = 0.87 V, chiral **4** had a similar E_1 and a different E_2. The $E_2 - E_1$ values of 3.19 V for (*P*)-**4** and (±)-**4** and of 3.40 V for pyrene indicated that the distortion reduced $E_2 - E_1$ by 0.21 V.

Table 3. Oxidation and Reduction Potentials of Pyrene Derivatives in 0.1 M n-Bu_4NClO_4/Acetonitrile Solution

	E_1[a] (V vs Fc^+/Fc)	E_2[a] (V vs Fc^+/Fc)	$E_2 - E_1$ (V)	difference from pyrene (V)
pyrene	−2.53	0.87	3.40	0
(±)-**4**	−2.57	0.62	3.19	−0.21
(*P*)-**4**	−2.57	0.62	3.19	−0.21

[a]Determined by DPV.

The distortion of equatorenes facilitated oxidation but hardly affected reduction, which was due to the destabilized HOMO energy level and relatively unaffected LUMO energy level. Such properties would generally be observed in equatorenes.

CALCULATIONS

DFT calculations were conducted for naphthalene, 1,8-dimethylnaphthalene, 1,8-diisopropylnaphthalene, 1,8-di(*t*-butyl)naphthalene, and **1**, in order to compare the effects of the substituents (Table 4). The molecular structures were optimized at the B3LYP/6-31G(d) level in vacuum, and absorption spectra were calculated within a time-dependent DFT framework using the PBE0 hybrid functional with the 6-311G(d,p) basis set.[15] All the DFT calculations were carried out using the Gaussian 09 program package.[16] The calculations showed that naphthalene and 1,8-dimethylnaphthalene have flat structures, and distorted structures were obtained for their derivatives with isopropyl and larger 1,8-substituents, which were consistent with the X-ray structure.[4c,17] The calculated structure of **1** well reproduced the experimental structures obtained by X-ray analysis. For example, the dihedral angle H/C−C1−C8−H/C of 71.6° was obtained experimentally for (±)-**1**, and that of 72.2° was obtained by calculation. The calculated UV−vis absorption maximum of 326 nm coincided with the experimental maximum of 323 nm. The difference in the HOMO−LUMO gap between **1** and naphthalene was calculated to be 0.58 eV, which was in good agrrement with the experimental $E_2 - E_1$ of 0.45 eV obtained by the electrochemical analysis. Compared with that of naphthalene, the HOMO energy level of **1** was destabilized by the introduction of 1,8-bis(1-adamantyl) substituents, whereas the LUMO energy level showed a small change.[18] These were also consistent with the result of the electrochemical analysis.

DFT calculations were also conducted for pyrene and **4** (Table 5). The experimental dihedral angle H/C−C3−C4−H/C of 77.8° obtained by X-ray analysis of (±)-**4** was in agreement with the

Table 4. Results of Calculations for Naphthalene and 1,8-Disubstituted Naphthalenes

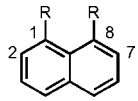

R	H	Me	*i*-Pr	*t*-Bu	1-Ad (**1**)
symmetry	D_{2h}	C_{2v}	C_2	C_2	C_1[b]
sum of the bond angles at 1,8-carbon	360.0	360.0	359.8	357.7	357.6
dihedral angle					
H/C−C1−C8−H/C	0.0	0.0	27.4	70.1	72.2
H/C−C2−C7−H/C	0.0	0.0	25.1	63.2	65.1
absorption (nm) (oscillation strength in parentheses)	276 (0.064)	285 (0.099)	295 (0.112)	321 (0.090)	326 (0.101)
HOMO (eV)[a]	−5.79	−5.50	−5.45	−5.30	−5.23
LUMO (eV)[a]	−0.96	−0.80	−0.87	−1.01	−0.98
LUMO − HOMO (eV)	4.83	4.70	4.58	4.29	4.25
difference from naphthalene (eV)	0	−0.13	−0.25	−0.54	−0.58

[a]HOMO and LUMO energy levels were derived from B3LYP/6-31G(d) calculations. [b]The optimized geometry was very close to C_2 symmetry structure.

dx.doi.org/10.1021/ja407800e | J. Am. Chem. Soc. 2013, 135, 16526−16532

Table 5. Results of Calculations for Pyrene and 4

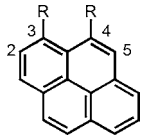

R	H	1-Ad (**4**)
symmetry	D_{2h}	C_1
sum of the bond angles at 3,4-carbon	360.0	358.0, 357.4
dihedral angle		
H/C−C3−C4−H/C	0.0	73.6
H/C−C2−C5−H/C	0.0	67.1
absorption (nm) (oscillation strength in parentheses)	330 (0.271)	366 (0.285)
HOMO (eV)[a]	−5.33	−5.00
LUMO (eV)[a]	−1.48	−1.41
LUMO − HOMO (eV)	3.85	3.58
difference from pyrene (eV)	0	−0.27

[a]HOMO and LUMO energy levels were derived from B3LYP/6-31G(d) calculations.

calculated value of 73.6°. The calculated UV−vis absorption maximum of 366 nm coincided with the experimental value of 362 nm. The difference in the HOMO−LUMO gap between **4** and pyrene was calculated to be 0.27 eV, which was in good agreement with the experimental $E_2 - E_1$ of 0.21 eV obtained by the electrochemical analysis. The HOMO energy level of **4** was destabilized compared with that of pyrene, and the LUMO energy level of **4** showed a small change compared with that of pyrene. These were also consistent with the result of the electrochemical analysis. The effect of distortion on the aromatic π systems of naphthalenes and pyrenes appears to be a common feature of equatorenes.

To determine the origin of the different effects of distortion on the HOMO and LUMO in **1**, the structures of the HOMO and LUMO were compared between naphthalene and **1** (Figure 10). The LUMO had similar structures on the naphthalene ring for both compounds, which was consistent with the small differences in LUMO energy level between naphthalene and **1**. As for the HOMO, the pseudo-π-conjugation,[19] mixing of the σ-orbitals of the adamantyl group with the aromatic π-orbitals, was substantial in **1**, differently from naphthalene. The apparent mixing of the aromatic π-system with the σ-orbitals in the adamantyl moiety in **1** reduced the aromaticity of the HOMO, which induced the destabilization of the HOMO energy level. Perturbation by distortion depends on the orbitals, which exert different spectroscopic properties.

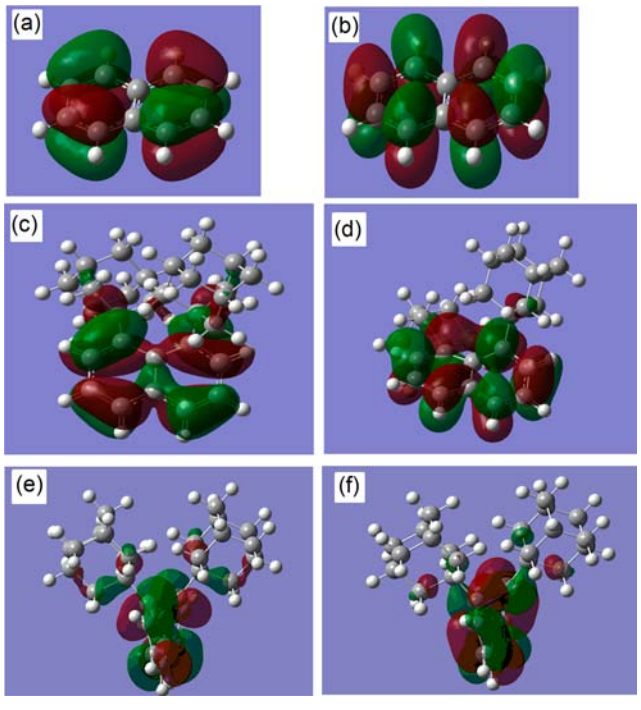

Figure 10. HOMOs (a, c, and e) and LUMOs (b, d, and f) of naphthalene and **1** calculated at the B3LYP/6-31G(d) level.

CONCLUSION

In summary, a series of chiral naphthalene, phenanthrene, chrysene, and pyrene with bis(1-adamantyl) groups at the peri-position were synthesized in optically pure form, which did not at all racemize at ambient temperature. X-ray analysis showed that the naphthalene moiety attached to the bis(1-adamantyl) group of equatorenes is distorted, and that the other aromatic rings have flat structures. The physical properties of the equatorenes are different from those of the original arenes lacking the adamantyl groups: UV−vis showed a considerable redshift in the absorption maximum; a very weak fluorescence was observed; the distortion destabilized the HOMO but hardly affected the LUMO; the aromatic π-system was extended to the adamantyl group in the HOMO. Note that equatorenes can be exploited in the devlopment of various chiral versions of aromatic compounds exhibiting notable functions.

ASSOCIATED CONTENT

Supporting Information

Experimental details, synthetic conditions, chiral HPLC analyses of equatorenes (Figures S2−S5), kinetic study about the racemization of (*P*)-**1**, (*P*)-**2**, (*P*)-**3**, and (*P*)-**4** (Figures S6−S9), UV−vis and fluorescence spectra of (±)-**2**, (*P*)-**2**, and phenanthrene (Figures S10 and S11), UV−vis and fluorescence spectra of (±)-**3**, (*P*)-**3**, and chrysene (Figures S12 and S13), fluorescence spectra of (±)-**4**, (*P*)-**4**, and pyrene (Figure S14), electrochemical analysis of (±)-**1**, (*P*)-**1**, naphthalene, 1,8-dimethylnaphthalene, (±)-**4**, (*P*)-**4**, and pyrene (Figures S15−S21), experimental values of calculations on 1,8-disubstituted naphthalene derivatives, **1**, and **4**, crystallographic data of (±)-**1**, (±)-**2**, (±)-**3**, (±)-**4**, and (±)-*anti*-**8** (Tables S1−S5), their CIF files giving crystal data, and copies of ^{1}H and ^{13}C NMR spectra of all new compounds. This material is available free of charge via the Internet at http://pubs.acs.org.

AUTHOR INFORMATION

Corresponding Author

yama@m.tohoku.ac.jp

Notes

The authors declare no competing financial interest.

ACKNOWLEDGMENTS

The authors thank Dr. Umpei Nagashima (Nanosystem Research Institute, AIST) for helpful discussions in interpreting our theoretical calculations. Financial support in the form of a Grant-in-Aid for Scientific Research (No. 21229001) from the Japanese Ministry of Education, Culture, Sports, Science and Technology is acknowledged. A fellowship from the Japan Society for the Promotion of Science for young Japanese scientists to K.Y. is also acknowledged.

REFERENCES

(1) *Polycyclic Aromatic Hydrocarbons*; Harvey, R. G., Ed.;Wiley-VHC: New York, 1997.

(2) Recent Reviews of Helicenes: (a) Shen, Y.; Chen, C.-F. *Chem. Rev.* **2012**, *112*, 1463−1535. (b) Gingras, M. *Chem. Soc. Rev.* **2013**, *42*, 968−1006. (c) Gingras, M.; Félix, G.; Peresutti, R. *Chem. Soc. Rev.* **2013**, *42*, 1007−1050. (d) Gingras, M. *Chem. Soc. Rev.* **2013**, *42*, 1051−1095.

(3) Pradhan, A.; Dechambenoit, P.; Bock, H.; Durola, F. *J. Org. Chem.* **2013**, *78*, 2266−2274.

(4) 1,8-Di-(*tert*-butyl)naphthalene derivatives: (a) Franck, R. W.; Leser, E. G. *J. Org. Chem.* **1970**, *35*, 3932−3939. (b) Anderson, J. E.; Franck, R. W.; Mandella, W. L. *J. Am. Chem. Soc.* **1972**, *94*, 4608−4614. (c) Handal, J.; White, J. G.; Franck, R. W.; Yuh, Y. H.; Allinger, N. L. *J. Am. Chem. Soc.* **1977**, *99*, 3345−3349. (d) Anderson, J. E.; Franck, R. W. *J. Chem. Soc., Perkin Trans. 2* **1984**, 1581−1582.

(5) Recent reports on distorted naphthalenes with large substituents, except alkyl groups, at peri-position: (a) Cohen, S.; Thirumalaikumar, M.; Pogodin, S.; Agranat, I. *Struct. Chem.* **2004**, *15*, 339−346. (b) Killan, P.; Slawin, A. M. Z.; Woollins, J. D. *Inorg. Chim. Acta* **2005**, *358*, 1719−1723. (c) Aucott, S. M.; Duerden, D.; Li, Y.; Slawin, A. M. Z.; Woollins, J. D. *Chem.—Eur. J.* **2006**, *12*, 5495−5504. (d) Ozeryanskii, V. A.; Pozharskii, A. F.; Artaryan, A. K.; Vistorobskii, N. V.; Starikova, Z. A. *Eur. J. Org. Chem.* **2009**, 1241−1248.

(6) Distorted naphthalenes with the group 14 element at peri-position: (a) Seyferth, D.; Vick, S. C. *J. Organomet. Chem.* **1977**, *141*, 173−187. (b) Hutchings, M. G.; Watt, I. *J. Organomet. Chem.* **1979**, *177*, 329−332. (c) Blount, J. F.; Cozzi, F.; Damewood, J. R., Jr.; Iroff, L. D.; Sjöstrand, U.; Mislow, K. *J. Am. Chem. Soc.* **1980**, *102*, 99−103. (d) Soorlyakumaran, R.; Boudjouk, P. *Organometallics* **1982**, *1*, 218−219. (e) Nori-Shargh, D.; Amini, M. M.; Jameh-Bozorghi, S. *Phosphorus, Sulfur Silicon Relat. Elem.* **2003**, *178*, 2529−2537. (f) Nori-Shargh, D.; Malekhosseini, M.; Deyhimi, F. *J. Mol. Struct.* **2006**, *763*, 187−198.

(7) Examples of distorted acenes that bear several bulky substituents or multiple benzoannulations: (a) Qiao, X.; Padula, M. A.; Ho, D. M.; Vogelaar, N. J.; Schutt, C. E.; Pascal, R. A., Jr. *J. Am. Chem. Soc.* **1996**, *118*, 741−745. (b) Lu, J.; Ho, D. M.; Vogelaar, N. J.; Kraml, C. M.; Bernhard, S.; Byrne, N.; Kim, L. R.; Pascal, R. A., Jr. *J. Am. Chem. Soc.* **2006**, *128*, 17043−17050. Review: (c) Pascal, R. A., Jr. *Chem. Rev.* **2006**, *106*, 4809−4819.

(8) Examples of naphthalenes with cyclophane structure: (a) Otsubo, T.; Aso, Y.; Ogura, F.; Misumi, S.; Kawamoto, A.; Tanaka, J. *Bull. Chem. Soc. Jpn.* **1989**, *62*, 164−170. (b) Tobe, Y.; Takahashi, T.; Ishikawa, T.; Yoshimura, M.; Suwa, M.; Kobiro, K.; Kakiuchi, K.; Gleiter, R. *J. Am. Chem. Soc.* **1990**, *112*, 8889−8894.

(9) Aikawa, H.; Takahira, Y.; Yamaguchi, M. *Chem. Commun.* **2011**, *47*, 1479−1481.

(10) Kajigaeshi, S.; Kakinami, T.; Tokiyama, H.; Hirakawa, T.; Okamoto, T. *Bull. Chem. Soc. Jpn.* **1987**, *60*, 2667−2668.

(11) Ireland, R. E.; Walba, D. M. *Org. Synth.* **1977**, *56*, 44. *Org. Synth. Collect. Vol. VI*, **1988**, 567.

(12) (a) Fürstner, A.; Mamane, V. *J. Org. Chem.* **2002**, *67*, 6264−6267. (b) Fürstner, A.; Mamane, V. *Chem. Commun.* **2003**, 2112−2113. (c) Mamane, V.; Hannen, P.; Fürstner, A. *Chem.—Eur. J.* **2004**, *10*, 4556−4575. (d) Wu, A.; Xu, D.; Lu, D.; Penning, T. M.; Blair, I. A.; Harvey, R. G. *Tetrahedron* **2012**, *68*, 7217−7233.

(13) Yadokari-XG, Software for Crystal Structure Analyses, Wakita, K. (2001); Release of Software (Yadokari-XG 2009) for Crystal Structure Analyses. Kabuto, C.; Akine, S.; Nemoto, T.; Kwon, E. *J. Cryst. Soc. Jpn.* **2009**, *51*, 218.

(14) Tan, Z.; Kote, R.; Samaniego, W. N.; Weininger, S. J.; McGimpsey, W. G. *J. Phys. Chem. A* **1999**, *103*, 7612−7620.

(15) Adamo, C.; Barone, V. *J. Chem. Phys.* **1999**, *110*, 6158−6170.

(16) Frisch, M. J.; Trucks, G. W.; Schlegel, H. B.; Scuseria, G. E.; Robb, M. A.; Cheeseman, J. R.; Scalmani, G.; Barone, V.; Mennucci, B.; Petersson, G. A.; Nakatsuji, H.; Caricato, M.; Li, X.; Hratchian, H. P.; Izmaylov, A. F.; Bloino, J.; Zheng, G.; Sonnenberg, J. L.; Hada, M.; Ehara, M.; Toyota, K.; Fukuda, R.; Hasegawa, J.; Ishida, M.; Nakajima, T.; Honda, Y.; Kitao, O.; Nakai, H.; Vreven, T.; Montgomery, Jr., J. A.; Peralta, J. E.; Ogliaro, F.; Bearpark, M.; Heyd, J. J.; Brothers, E.; Kudin, K. N.; Staroverov, V. N.; Kobayashi, R.; Normand, J.; Raghavachari, K.; Rendell, A.; Burant, J. C.; Iyengar, S. S.; Tomasi, J.; Cossi, M.; Rega, N.; Millam, J. M.; Klene, M.; Knox, J. E.; Cross, J. B.; Bakken, V.; Adamo, C.; Jaramillo, J.; Gomperts, R.; Stratmann, R. E.; Yazyev, O.; Austin, A. J.; Cammi, R.; Pomelli, C.; Ochterski, J. W.; Martin, R. L.; Morokuma, K.; Zakrzewski, V. G.; Voth, G. A.; Salvador, P.; Dannenberg, J. J.; Dapprich, S.; Daniels, A. D.; Farkas, Ö.; Foresman, J. B.; Ortiz, J. V.; Cioslowski, J.; Fox, D. J. *Gaussian 09*, revision C.01; Gaussian, Inc.: Wallingford CT, 2009.

(17) Naphthalene: (a) Cruickshank, D. W. J.; Sparks, R. A. *Proc. R. Soc. A* **1960**, *258*, 270−285. 1,8-Dimethylnaphthalene: (b) Wilson, C. C.; Nowell, H. *New. J. Chem.* **2000**, *24*, 1063−1066.

(18) Calculations of polymethylated naphthalenes were reported, which noted redshifts of UV−vis and destabilized HOMO. Mora-Diez, N.; Boyd, R. J.; Heard, G. L. *J. Phys. Chem. A* **2000**, *104*, 1020−1029.

(19) Nagaoka, S.; Okauchi, Y.; Urano, S.; Nagashima, U.; Mukai, K. *J. Am. Chem. Soc.* **1990**, *112*, 8921−8924.